研究成果の刊行に関する一覧表

書籍

著者氏名	論文タイトル名	書籍全体の編集者名	書　籍　名	出版社名	出版地	出版年	ページ
工藤幸司	分子イメージング	平井俊策	老年期認知症ナビゲーター	メディカルビュー社	東京	2006	248-249

雑誌

発表者氏名	論文タイトル名	発表誌名	巻	ページ	出版年
Kudo Y	Development of amyloid imaging PET probes for an early diagnosis of Alzheimer's disease	Minimally Invasive Therapy and Applied Technology	15	209-213	2006
Ishikawa K, Kudo Y, Nishida N, Suemoto T, Sawada T, Iwaki T, Doh-ura K	Styrylbenzoxazole derivatives for imaging of prion plaques and treatment of transmissible spongiform encephalopathies	J Neurochem. 99: 198-205. 2006	99	198-205	2006
Fujiwara H, Iwasaki K, Furukawa K, Seki T, He M, Maruyama M, Tomita N, Kudo Y, Higuchi M, Saido TC, Maeda S, Takashima A, Hara M, Ohizumi Y, Arai H	Uncaria rhynchophylla, a Chinese medicinal herb, has potent antiaggregation effects on Alzheimer's beta-amyloid proteins.	J Neurosci Res	84	427-433	2006
Doh-ura K, Tamura K, Karube Y, Naito M, Tsuruo T, Kataoka Y	Chelating compound, chrysoidine, is more effective in both anti-prion activity and brain endothelial permeability than quinacrine	Cell. Mol. Neurobiol.		in press	
Fukuuchi T, Doh-ura K, Yoshihara S, Ohta S	Metal complexes with superoxide dismutase-like activity as candidates for anti-prion drug.	Bioorg. Med. Chem. Lett.	16	5982-5987	2006
Sasaki K, Doh-ura k, : Ironside J, Mabbott N, Iwaki T	Clusterin expression in follicular dendritic cells associated with prion protein accumulation.	J. Pathol.	209	484-491	2006

Wakisaka Y, Santa N, Doh-ura K, Kitamoto T, Ibayashi S, Iida M, Iwaki T	Increased asymmertric pulvinar magnetic resonance imaging signals in Creutzfeldt-Jakob disease with florid plaques following a cadaveric dura mater graft	Neuropathol.	26	82-88	2006
Shintaku M, Yutani C, Doh-ura K	Brain stem lesions in sporadic Creutzfeldt-Jakob disease: A histopathological and immunohistochemical study	Neuropathol.	26	43-49	2006
Kawatake S, Nishimura Y, Sakaguchi S, Iwaki T, Doh-ura K	Surface plasmon resonance analysis for the screening of anti-prion compounds.	Biol. Pharm Bull.	29	927-932	2006
荒井啓行、工藤幸司	認知症診断に役立つ補助検査法－生物学的診断マーカーと脳分子イメージング	Cognition and Dementia.	5	101-105	2006
工藤幸司	PET によるアミロイドイメージング	Medical Practice	23	1183-1184	2006
工藤幸司、荒井啓行	脳アミロイドの分子イメージング	Curerent Insights in Neurological Science	14	8-9	2006
岡村信行、谷内一彦、古本祥三、工藤幸司、荒井啓行	脳内アミロイドβ蛋白およびタウ蛋白の PET イメージング技術の開発.	Innervision	21	43	2006
工藤　幸司	軽度認知障害—アルツハイマー型認知症の初期、その前駆状態を中心に 「今後の画像診断」.	Modern Physician	26	1835-1838	2006
岡村信行、古本祥三、工藤幸司、谷内一彦	臨床応用　脳の分子イメージング「アルツハイマー病」	日本臨床	65	320-326	2006
岡村信行、谷内一彦、工藤幸司	アミロイドイメージングの進歩	Dementia Japan	20	216-225	2007

古川勝敏、温　世栄、岡村信行、工藤幸司、荒井啓行	アルツハイマー病におけるシナプス障害.	Dementia Japan	20	253-261	2007
荒井啓行、工藤幸司	病理像を画像化する分子神経イメージング法によるAlzheimer病の早期診断-日本での BF-227 の開発と臨床応用	医学のあゆみ	220	404-408	2007
岡村信行	老人斑および神経原線維変化の非侵襲的検出を目的とした新規 PET プローブの開発研究	東北医学雑誌	118	143-147	2006
岡村信行	アルツハイマー病と関連疾患の画像診断 その未来	クリニシアン	53	932-937	2006
福田寛、岡村信行	分子イメージング総論	BRAIN and Nerve	59	203-207	2007
逆瀬川裕二、堂浦克美.	プリオン病の治療 —その現状と展望—	Brain Medical	18	356-370	2006
逆瀬川裕二、堂浦克美	孤発性クロイツフェルト・ヤコブ病と6種類のサブタイプ	Medical Briefs in Brain & Nerve	15	5-6	2006
石川謙介、堂浦克美	プリオンイメージングの試み.	Clinical Neuroscience	24	313-316	2006

研究成果の刊行物・別刷

分子イメージング

工藤幸司

Aβと標識プローブ結合を *in vivo* で画像化し，診断しようとするのがアミロイドイメージングである．すでにいくつかのプローブの探索的臨床試験が実施されており，AD の早期，鑑別，発症前診断などを可能にすると考えられている．

はじめに

AD においては患者を取り巻く家族，または臨床家がこの疾患特有の臨床症状に気づいたときには，それぞれ Aβ および過剰リン酸化タウ蛋白を主構成成分とする老人斑および神経原線維変化などの病理像はもはや取り返しのつかないほど進行していることが知られている．すなわち，現状の AD 診断を癌のそれに例えるなら，末期状態に達した時点でしか検出されていないことになる．近年，一部 AD の前駆状態と考えられている MCI においても病理学的にはすでに立派な AD 状態であることが明らかにされていることから，AD はもの忘れ症状が発現するかなり以前からその病理像がスタートしていることになる．これらの事実は AD の臨床像と病理像，言い換えると clinical AD と pathological AD との間には大きな乖離が存在することを示唆している．

本項で紹介する Aβ 分子を画像化するアミロイドイメージングは，AD の病理像としてのβシート構造をとった Aβ を追跡することから，診断原理的に早期，鑑別，さらに発症前診断をも可能とすると考えられている．

それでは，アミロイドイメージングとはいかなるストラテジーに基づくかについて解説すると概念は以下の通りである．

①AD の病理学的主徴の 1 つ，老人斑のほとんどはβシート構造をとった Aβ によって形成されている．

②同シート構造をとった Aβ に特異的選択的に結合し，かつ容易に血液－脳関門を透過する低分子有機化合物を見出す．

③この化合物を PET または SPECT で扱うことが可能な核種で標識する．

④これをプローブとして生体に静脈内投与する．

⑤プローブは血液－脳関門を越えて脳内の老人斑を形成している Aβ に結合する．一定時間後には非結合プローブは洗い流され，Aβ に結合したプローブのみが脳内に残る．

⑥これを PET または SPECT を用い，イメージング画像として取り込み，βシート構造をとった脳内 Aβ(＝老人斑)蓄積量の定量およびその空間的分布から AD を診断する．

AD 診断用プローブ

アミロイドイメージングを具体化させる最も高いハードルはβシート構造をとった Aβ に特異的選択的に結合し，かつ血液－脳関門を容易に透過し，さらに標的以外からは速やかにクリアランスされるなどの優れた特性を有するプローブを見出すことにある．これまで多くのプローブ候補化合物が報告されてきたが，これらの中で [^{18}F] FDDNP[1]，[^{11}C] PIB[2]，[^{11}C] SB-13[3]の 3 つの PET 用プローブが探索的臨床研究に供されている．これらの中で最も進捗度の高いピッツバーグ大学の Klunk らによって開発された [^{11}C] PIB について概説すると，AD 患者脳において高い集積の認め

用語解説 ——βシート構造

蛋白の高次構造の 1 つで，紙を蛇腹状に折りたたみ引き伸ばしたような状態．互いに隣接するペプチド鎖の NH 基と CO 基間で水素結合し，その結合が構造の安定化に寄与していると考えられている．

Recommended Readings

❶ Neurobiol Aging 19 : No.2, 1998

❷ Klunk WE et al : Ann Neurol 55 : 306-319, 2004

❸ Okamura N et al : J Neurosci 24 : 2535-2541, 2004

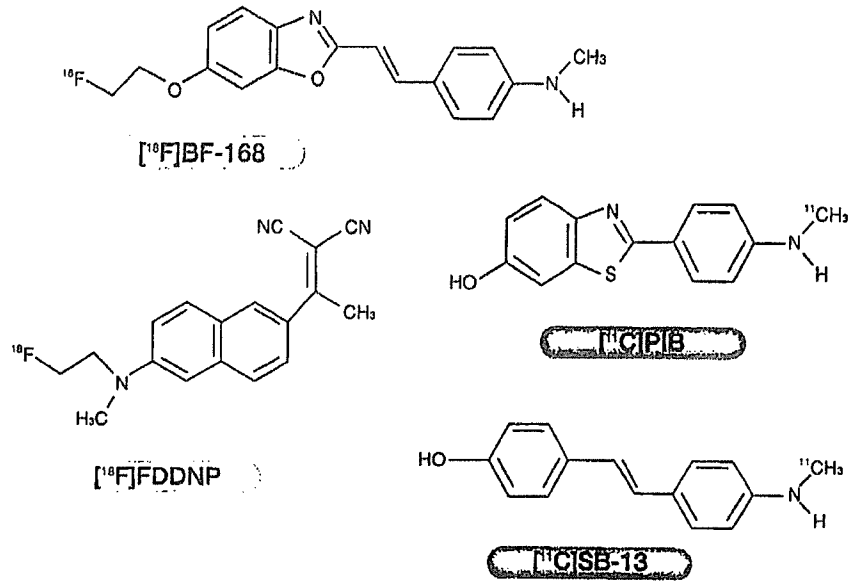

図　これまで報告されている代表的なアルツハイマー病診断用プローブ

られる部位は前頭葉，側頭頭頂葉などであるが，これらは明らかに健常コントロール画像と異なっており，また［^{18}F］FDG代謝の低下している部位に集積がみられた．［^{11}C］PIB集積のStandardized Uptake Value(SUV)と［^{18}F］FDGの代謝率を比較したところ，前者のSUVのほうが後者の代謝率よりもAD患者－健常コントロール間のデータのオーバーラップが少なかった．このことはこのプローブによる診断のほうが［^{18}F］FDGを用いたそれよりもADの診断精度が優れていることを示唆している．しかし一方，AD患者において［^{11}C］PIB集積が正常レベルであった例，正常コントロールでも集積の高かった例などもみられている．これらがfalse positve/negativeなのか，または発症前高リスク者であったのかは今後多例数を重ねて検討する必要があろう．

［^{11}C］SB-13[3]は［^{11}C］PIBとほとんど同じ成績であったことが報告されているが，［^{18}F］FDDNP[1]はかなり非特異的結合が多いことが知られている．

わが国発のプローブ

日本においては筆者らによって開発された老人斑に選択性の高いBF-168[4]のさらなる進化体であるBF-227(THK-002)と呼ばれるプローブの探索的臨床研究が，東北大学チームによって平成17年度から開始される予定である．

AD診断のガイドライン的な役割を果たしているのが，いわゆるレーガン研究所の有名なConsensus Report[5]である．同Reportが求めているのは，診断の感度および特異度はいずれも80％以上，陽性的中率は90％である．これまでのプローブの感度などのデータはまだ報告されていないが，診断原理的にこれまでの診断法のそれらを凌ぐことが予想される．

アミロイドイメージングと，近年開発されつつあるワクチンなどの根本療法とを組み合わせることにより，診断時点で発症前でさえあればADに罹患せずに一生を送らせることを可能とする時代の足音が聞こえている．

References
1) Shoghi-Jadid K et al : Am J Geriatr Psychiatry 10 : 24-35, 2002
2) Klunk WE et al : Ann Neurol 55 : 306-319, 2004
3) Verhoeff NP et al : Am J Geriatr Psychiatry 12 : 584-595, 2004
4) Okamura N et al : J Neurosci 24 : 2535-2541, 2004
5) Neurobiol Aging 19 : No.2, 1998

関連事項
アルツハイマー型認知症(痴呆) ▶▶ 96頁
老人斑 ▶▶ 212頁
βアミロイド前駆体蛋白(APP)とβアミロイド ▶▶ 216頁
PET ▶▶ 246頁
診断マーカー ▶▶ 252頁

ロウネン キ ニン チ ショウ
老年期認知症ナビゲーター

定価　本体4700円(税別)

2006年9月10日　第1版第1刷発行©

監修者　平井俊策(ヒライ シュンサク)
編集者　荒井啓行(アライ ヒロユキ)／浦上克哉(ウラカミカツヤ)／武田雅俊(タケダ マサトシ)／本間　昭(ホンマ アキラ)
発行者　松岡光明
発行所　株式会社メディカルレビュー社

〒113-0034　東京都文京区湯島3-19-11　イトーピア湯島ビル
電話/03-3835-3041(代)
編集部　電話/03-3835-3043　FAX/03-3835-3040
✉ editor-1@m-review.co.jp
販売部　電話/03-3835-3049　FAX/03-3835-3075
✉ sales@m-review.co.jp
〒541-0046　大阪市中央区平野町1-7-3　吉田ビル
電話/06-6223-1468(代)　振替　大阪6-307302
http://www.m-review.co.jp

印刷・製本／図書印刷株式会社
用紙／株式会社松菱洋紙店
本書に掲載された著作物の複写・複製・転載・翻訳・データベースへの取り込みおよび送信(送信可能化権を含む)・上映・譲渡に関する許諾権は㈱メディカルレビュー社が保有しています.
JCLS <㈱日本著作出版権管理システム委託出版物>
本書の無断複写は著作権法上での例外を除き，禁じられています．複写される場合は，そのつど事前に㈱日本著作出版権管理システム(電話03-3817-5670)の許諾を得てください.
乱丁・落丁の際はお取り替えいたします。

ISBN 4-7792-0015-6　C3047

Minimally Invasive Therapy. 2006; 15:4; 209–213

Taylor & Francis
Taylor & Francis Group

ORIGINAL ARTICLE

Development of amyloid imaging PET probes for an early diagnosis of Alzheimer's disease

YUKITSUKA KUDO

Tohoku University Biomedical Engineering Research Organization (TUBERO), Sendai, Japan

Abstract
Progressive accumulation of senile plaques (SPs) is one of the major neuropathological features of Alzheimer's Disease (AD) that precedes cognitive decline. Noninvasive detection of SPs could, therefore, be a potential diagnostic test for early or presymptomatic detection of AD patients. For this purpose, many attempts have been made to visualize AD-specific pathological changes in the living brain. Currently, a most practical method for the *in vivo* measurement of SP depositions is using positron emission tomography (PET) and contrast agent that specifically label SPs. We have developed a novel compound 2-[2-(2-dimethylaminothiazol-5-yl) ethenyl]-6-[2-(fluoro)ethoxy] benzoxazole (BF-227) as a candidate for an amyloid imaging probe for PET. BF-227 displayed high affinity to synthetic amyloid β fibrils and clearly stained both SPs and diffuse plaques in AD brain sections. Intravenous administration of [^{11}C]BF-227 into normal mice indicated that this labeled tracer readily penetrated the blood brain barrier (BBB) and was washed out quickly from brain tissue. Currently, we have investigated the clinical trial of [^{11}C]BF-227 in healthy subjects and AD patients.

Key words: *Alzheimer's disease, early diagnosis, amyloid imaging probes, senile plaques, positron emission tomography*

Introduction

Alzheimer's disease (AD) is the most prevalent cause of dementia characterized by irreversible impairment of the cognitive function with accumulation of senile plaques (SPs) and neurofibrillary tangles (NFTs). It is well known that the pathological features in AD brains, especially accumulation of SPs, precede the clinical symptoms by more than a decade. These several lines of evidence indicate the existence of a temporally wide dissociation between the clinical and neuropthological features of AD. Direct imaging of SPs in patients with AD *in vivo* would be very useful for the early or presymptomatic diagnosis of AD.

For early diagnosis of AD, several imaging techniques have been developed that can noninvasively detect SPs in the brain using positron emission tomography (PET), single photon emission computed tomography (SPECT), and magnetic resonance imaging (MRI).

SPs are composed of the amyloid-β protein (Aβ), which is proteolytically cleaved from amyloid precursor proteins (1). NFTs, in contrast, are composed of phosphorylated tau(2). Many attempts have been made to visualize AD-specific pathological changes in the living brain. Currently, a most practical method for the *in vivo* measurement of SP depositions uses PET and a contrast agent that specifically labels SPs (3). The development of amyloid imaging agents starts with Cong-red and thioflavin-T, which have been commonly used for histochemical staining of amyloid. However, these agents lack some characteristics for suitable amyloid imaging probes as shown in Table I. In the past 10 years many candidate agents have been developed for amyloid imaging probes with different chemical structures and properties (Figure 1). A Congo-red derivative, Chrysamine-G was first introduced as a candidate for an *in vivo* probe of amyloid deposition (4). As a consequence of compound optimization, (trans, trans)-1-bromo-2,5-bis-(3-hydroxycarbonyl-1,4-hydroxy) styrylbenzene

Correspondence: Y. Kudo, Tohoku University Biomedical Engineering Research Organization (TUBERO), 2-1, Seiryo-machi, Aoba-ku, Sendai, 980-8575, Japan. E-mail: kudoyk@tubero.tohoku.ac.jp

ISSN 1364-5706 print/ISSN 1365-2931 online © 2006 Taylor & Francis
DOI: 10.1080/13645700600836000

Table I. Requirements for amyloid imaging probes for clinical application

- High binding affinity to amyloid-β fibrils
- Selective binding to amyloid plaques
- High BBB permeability
- Fast clearance from normal brain tissue
- Metabolic stability
- Drug safety

(BSB) and methoxy-X04 have successfully visualized the brain amyloid deposits of APP transgenic mice after intravenous administration of these compounds (5,6).

The first clinical amyloid imaging of the brain of AD patients used [^{18}F] 2-(1-{ 6-[(2-fluoroethyl)-methyl-amino]-2-naphythyl } ethylidene) malononitrile ([^{18}F]FDDNP) (7). The following second and third imaging used *N*-methyl-[^{11}C]2-(4-methylaminophenyl)-6-hydroxybenzothiazole([^{11}C]PIB) and [^{11}C]4-N-methylamino-4-hydroxystilbene ([^{11}C]-SB-13), respectively(8,9).

However, FDDNP has some weakness in practical use due to their considerable amount of nonspecific accumulation in normal brain tissue (10).

Compared with controls, AD patients typically showed marked retention of [^{11}C]PIB in areas of association cortex known to contain large amounts of amyloid deposits in AD. In the AD patient group, PIB retention was increased most prominently in the frontal cortex. Large increases were also observed in parietal, temporal, and occipital cortices and the striatum. [^{11}C]PIB retention was equivalent in AD patients and controls in areas known to be relatively unaffected by amyloid deposition (such as subcortical white matter, pons, and cerebellum) (8). The high retention of [^{11}C]PIB in the frontal cortex conflicts with evidence from postmortem studies, in which the amyloid load is rarely highest in the frontal cortex (3).

Another amyloid imaging probe [^{11}C]SB-13 was also applied in a human PET study and exhibited binding properties similar to [^{11}C]PIB (9).

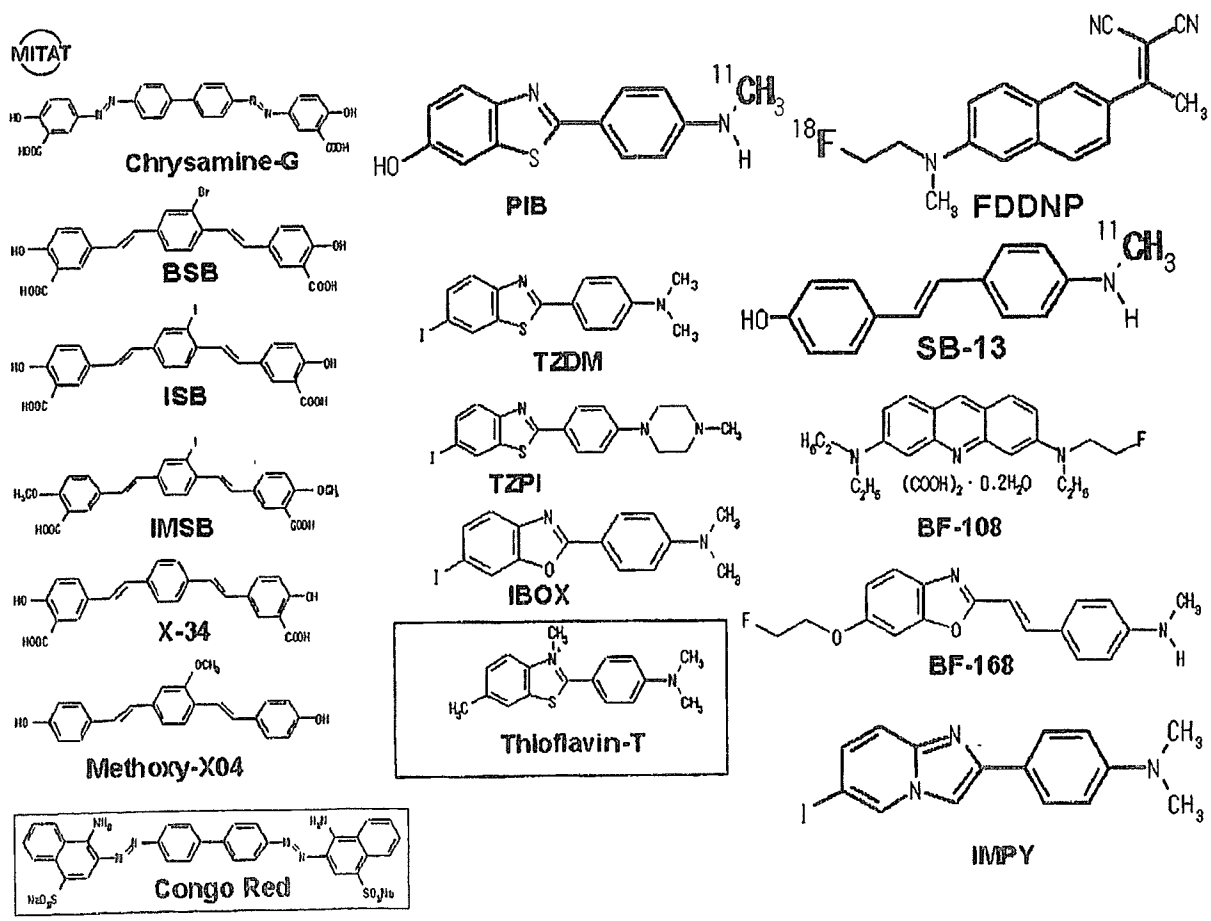

Figure 1. Chemical structures of imaging probes for *in vivo* detection of amyloid.

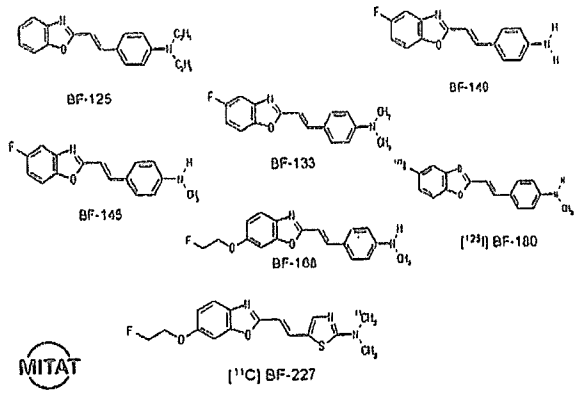

Figure 2. Chemical structures of our benzoxazole derivatives.

In Japan, our team has developed amyloid imaging probes since 1997 (Figure 2). We have previously reported a novel series of compounds including 6-(2-fluoroethoxy)-2-[2-(4-methylaminophenyl) ethenyl]-benzoxazole (BF-168), [2-(4-methylaminophenyl) ethenyl]-5-fluorobenzoxazole (BF-145) as promising candidates for *in vivo* imaging probes of SPs(11–13). These benzoxazole derivatives showed comparatively high permeability of blood-brain barrier (BBB), high affinity for Aβ aggregates, and high specificity for amyloid plaques including diffuse plaques, which suggests potential merit for detection of AD-related pathology. However, for application of these derivatives in a clinical PET study, we need to optimize the pharmacokinetic and safety of these molecules, and introduce an optimized derivative 2-[2-(2-dimethylaminothiazol-5-yl) ethenyl]-6-[2-(fluoro)ethoxy] benzoxazole (BF-227) as a candidate probe for *in vivo* imaging of amyloid in humans.

Material and methods

Affinity for synthetic Aβ1-42

Binding affinity of BF-227 for synthetic Aβ1-42 aggregates was examined as reported previously (12). Briefly, the binding assay was performed by mixing aliquot of aggregated Aβ1-42 with ^{125}I-labeled BF-180 (Figure 2).

Neuropathological staining in AD brain section

Postmortem brain tissues from autopsy-conformed AD cases were obtained from Fukushi-mura Hospital (Toyohashi, Japan). Experiments were performed under regulations of the ethics committee of the BF Research Institute. Brain sections were immersed in 100 μM of BF-227 solution containing 50 % ethanol.

BBB permeability of [^{11}C]BF-227 in normal mice

Brain uptakes of BF-227 were measured using ^{11}C-labeled compound. [^{11}C]BF-227 was administerd into the tail vein of normal mice. The mice were then sacrificed by decapitation at 2 and 60 min post injection (p.i.). The brains were removed and weighted, and the radioactivity was counted with an automatic γ-counter.

Acute and subacute toxicity of BF-227

Non-GLP toxicity study was carried out using female and male mice.

Other actions of BF-227

Postmortem brain section from autopsy-conformed AD cases was immersed in saline containing [^{11}C]BF-227, dipped in water, washed with EtOH, dried, and an autoradiographic image of the dried section was obtained using BAS-5000 phosphrimaging system (Fujifilm, Japan).

Ex vivo plaque labeling with BF-227 was evaluated using PS1/APPsw double transgenic mice. A BF-227 solution was administered into the tail vein.

Results

Affinity for synthetic Aβ1-42

The Ki value for Aβ1-42 fibrils in competitive binding assay using [^{125}I]BF-180 was 4.3 ± 1.3 nM in BF-227 (Kd value of [^{125}I]BF-180: 10.8 ± 1.5nM). This result suggests that BF-227 has a high binding affinity for Aβ1-42 fibrils.

Neuropathological staining in AD brain section

BF-227 clearly stained many SPs and diffuse plaques. This staining pattern corresponded to that of Aβ immunostaining in the adjacent section (Figure 3).

BBB permeability of [^{11}C]BF-227 in normal mice

Intravenous administration of [^{11}C]BF-227 into normal mice indicated that this labeled tracer readily penetrated the BBB (7.9 %ID/g at 2 min p.i.) and was washed out quickly (0.64 %ID/g at 60 min p.i.) from brain tissue.

Acute and subacute toxicity of BF-227

In an acute toxicity study, the lethal dose of BF-227 was larger than 10mg/kg (i.v.) for male and female

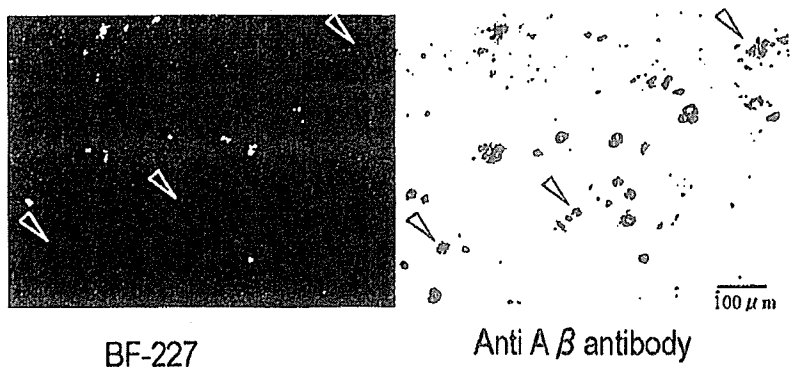

Figure 3. Neuropathological staining of amyloid plaques with BF-227 in AD brain sections. Sps and diffuse plaques (arrow head) were clearly stained with BF-227.

mice. In a subacute study, intravenous administration of BF-227 in tested doses did not produce any significant changes in general behavior and body weight. After 14 days post-treatment period, the mice did not show any microscopic alteration on pathological examination.

Other actions of BF-227

In the autoradiographic image using [^{11}C]BF-227, a specific binding pattern in the AD brain section was observed in the grey matter including SPs.

In the brain sections of PS1/APP Tg mice after intravenous injection of BF-227, numerous fluorescent spots were observed in the neocortex and hippocampus of the brain. These fluorescent spots corresponded to those of Aβ immunostaining in the same section.

Discussion and future prospects

BF-227 has high binding affinity to Aβ fibrils, remarkable stainability for SPs, high permeability of BBB, and fast clearance from normal brain tissue. The toxicity study of BF-227 indicates the sufficient safety margin of this compound for PET probe. Currently, we have investigated the clinical trial of [^{11}C]BF-227 in healthy subjects and in AD patients. This trial will elucidate the binding characteristics *in vivo* and the clinical usefulness of the probe in humans, and the results will be published by this summer or autumn.

Recently, we have introduced three novel compounds as candidate probes for *in vivo* imaging of tau pathology in the AD brain; 4-[2-(2-benzoimidazolyl) ethenyl]-N, N-diethylbenzenamine (BF-126), 2-[(4-methylamino) phenyl] quinoline (BF-158), and 2-(4-aminophenyl) quinoline (BF-170) (14) (Figure 4). In neuropathological examination,

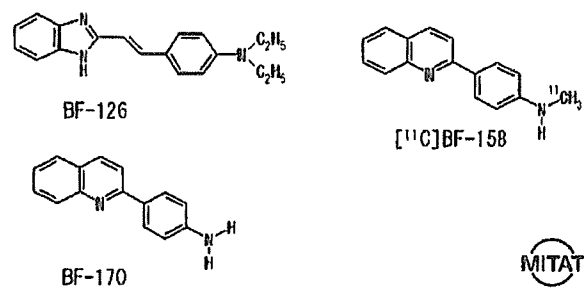

Figure 4. Chemical structures of our tau specific probes.

BF-126, BF-158, and BF-170 clearly stained NFTs, neuropil threads, and paired helical filament-type neuritis in the AD brain section. In addition, NFTs was labeled by 11C-labeled BF-158 with autoradiography. These findings suggest the potential usefulness of quinoline and benzimidazole derivatives for *in vivo* imaging of tau pathology in AD.

Several 11-C labeled probes for detecting SPs in AD patients have been reported from some teams. The short half-life (20 min) of 11-C, however, may limit the usefulness of these probes for a widespread application. Comparable 18-F labeled probes may supplant the clinical need due to the longer half-life of the isotope (109.7 min) (15). Further studies to develop 18-F labeled PET probes for the imaging of SPs are currently under way in some teams, including ours.

Unlike Alois Alzheimer, we now have access to instrumentation that allows visualization of the human brain *in vivo*. Brain imaging has become a part of the routine clinical assessment of dementia disorder (16). Recently, anti-amyloid agents such as Aβ vaccine and selective secretase inhibitors have been developed for the causal therapy of AD patients. AD patients all over the world may be

effectively diagnosed and treated by a combination of presymptomatic diagnosis and causal therapy.

Acknowledgement

The author thanks all the present and past members of our team and collaborators.

This study was financially supported by the Special Coordination Funds for Promoting Science and Technology, the Health and Labour Sciences Research Grants for Translational research from Ministry of Health, Labour and Welfare, Japan, the Program for Promotion of Fundamental Studies in Health Science of the National Institute of Biomedical Innovation, the New Energy and Industrial Technology Development Organization (NEDO), the Novartis foundation for Gerontological Research, the AstraZeneca Research Grant, and the Mitsui Sumitomo Insurance Welfare.

References

1. Shoji M, Golde TE, Ghiso J, Cheung TT, et al. Production of the Alzheimer amyloid beta protein by normal proteolytic processing. Science. 1992;258:126–9.
2. Lee VM, Balin BJ, Otvos L, Jr. Trojanowski JQ. A68: a major subunit of paired helical filaments and derivatized forms of normal Tau. Science. 1991;251:675–8.
3. Nordberg A. PET imaging of amyloid in Alzheimer's disease. Lancet Neurol. 2004;3:519–27.
4. Klunk WE, Debnath ML, Pettegrew JW. Chrysamine-G binding to Alzheimer and control brain: autopsy study of a new amyloid probe. Neurobiol Aging. 1995;16:541–8.
5. Skovronsky DM, Zhang B, Kung MP, Kung HF, et al. In vivo detection of amyloid plaques in a mouse model of Alzheimer's disease. Proc Natl Acad Sci U S A. 2000;97:7609–14.
6. Klunk WE, Bacskai BJ, Mathis CA, Kajdasz ST, et al. Imaging Abeta plaques in living transgenic mice with multi-photon microscopy and methoxy-X04, a systemically administered Congo red derivative. J Neuropathol Exp Neurol. 2002;61:797–805.
7. Shoghi-Jadid K, Small GW, Agdeppa ED, Kepe V, et al. Localization of neurofibrillary tangles and beta-amyloid plaques in the brains of living patients with Alzheimer disease. Am J Geriatr Psychiatry. 2002;10:24–35.
8. Klunk WE, Engler H, Nordberg A, Wang Y, et al. Imaging brain amyloid in Alzheimer's disease with Pittsburgh Compound-B. Ann Neurol. 2004;55:306–19.
9. Verhoeff NP, Wilson AA, Takeshita S, Trop L, et al. In-vivo imaging of Alzheimer disease beta-amyloid with [11C]SB-13 PET. Am J Geriatr Psychiatry. 2004;12:584–95.
10. Bacskai BJ, Klunk WE, Mathis CA, Hyman BT. Imaging amyloid-beta deposits in vivo. J Cereb Blood Flow Metab. 2002;22:1035–41.
11. Okamura N, Suemoto T, Shiomitsu T, Suzuki M, et al. A novel imaging probe for in vivo detection of neuritic and diffuse amyloid plaques in the brain. J Mol Neurosci. 2004;24:247–55.
12. Okamura N, Suemoto T, Shimadzu H, Suzuki M, et al. Styrylbenzoxazole derivatives for in vivo imaging of amyloid plaques in the brain. J Neurosci. 2004;24:2535–41.
13. Shimadzu H, Suemoto T, Suzuki M, Shiomitsu T, et al. Novel probes for imaging amyloid-beta: F-18 and C-11 labeling of 2-(4-aminostyryl)benzoxazole derivatives. Journal of Labelled Compounds & Radiopharmaceuticals. 2004;47:181–90.
14. Okamura N, Suemoto T, Furumoto S, Suzuki M, et al. Quinoline and benzimidazole derivatives: candidate probes for in vivo imaging of tau pathology in Alzheimer's disease. J Neurosci. 2005;25:10857–62.
15. Chandra R, Kung MP, Kung HF. Design, synthesis, and structure-activity relationship of novel thiophene derivatives for beta-amyloid plaque imaging. Bioorg Med Chem Lett. 2006;16:1350–2.
16. Nordberg A. Is amyloid plaque imaging the key to monitoring brain pathology of Alzheimer's disease in vivo? Eur J Nucl Med Mol Imaging. 2004;31:1540–3.

Journal of Neurochemistry, 2006, **99**, 198–205 doi:10.1111/j.1471-4159.2006.04035.x

Styrylbenzoazole derivatives for imaging of prion plaques and treatment of transmissible spongiform encephalopathies

Kensuke Ishikawa,* Yukitsuka Kudo,† Noriyuki Nishida,‡ Takahiro Suemoto,§ Tohru Sawada,§ Toru Iwaki¶ and Katsumi Doh-ura*

**Department of Prion Research, Tohoku University Graduate School of Medicine, Sendai, Japan*

†Division of Telecommunication and Information Technology, Biomedical Engineering Research Organization, Tohoku University, Sendai, Japan

‡Division of Cellular and Molecular Biology, Nagasaki University Graduate School of Biomedical Sciences, Nagasaki, Japan

§BF Research Institute Inc., Osaka, Japan

¶Department of Neuropathology, Graduate School of Medical Sciences, Kyushu University, Fukuoka, Japan

Abstract

Recent prevalence of acquired forms of transmissible spongiform encephalopathies (TSEs) has urged the development of early diagnostic measures as well as therapeutic interventions. To extend our previous findings on the value of amyloid imaging probes for these purposes, styrylbenzoazole derivatives with better permeability of blood–brain barrier (BBB) were developed and analyzed in this study. The new styrylbenzoazole compounds clearly labeled prion protein (PrP) plaques in brain specimens from human TSE in a manner irrespective of pathogen strain, and a representative compound BF-168 detected abnormal PrP aggregates in the brain of TSE-infected mice when the probe was injected intravenously. On the other hand, most of the compounds inhibited abnormal PrP formation in TSE-infected cells with IC_{50} values in the nanomolar range, indicating that they represent one of the most potent classes of inhibitor ever reported. BF-168 prolonged the lives of mice infected intracerebrally with TSE when the compound was given intravenously at the preclinical stage. The new compounds, however, failed to detect synaptic PrP deposition and to show pathogen-independent therapeutic efficacy, similar to the amyloid imaging probes we previously reported. The compounds were BBB permeable and non-toxic at doses for imaging and treatment; therefore, they are expected to be of practical use in human TSE.

Keywords: amyloid imaging, anti-prion activity, pathogen strain, prion disease, styrylbenzoazole derivatives.

J. Neurochem. (2006) **99**, 198–205.

The transmissible spongiform encephalopathies (TSEs) or prion diseases form a group of neurodegenerative disorders characterized by abnormal deposition of protease-resistant isoforms of prion protein (PrP) in the CNS (Prusiner 1991). TSEs are classified as sporadic, hereditary or environmentally acquired, and have become a serious public health issue because of the recent prevalence of acquired Creutzfeldt–Jakob disease (CJD), such as the variant form due to bovine spongiform encephalopathy (Will *et al.* 1996) and the iatrogenic form with cadaveric growth hormone or dura grafts (Brown *et al.* 2000). There is an urgent need to develop prophylactic and therapeutic interventions as well as diagnostic measures at the preclinical or early clinical stages of these incurable diseases.

We have previously reported that some amyloid imaging compounds, primarily derived from amyloid dyes such as

Received February 16, 2006; revised manuscript received May 25, 2006; accepted May 30, 2006.

Address correspondence and reprint requests to Dr Kensuke Ishikawa, Division of Prion Biology, Department of Prion Research, Tohoku University Graduate School of Medicine, 2–1 Seiryo-machi, Aoba-ku, Sendai 980-8575, Japan. E-mail: ishikawa@mail.tains.tohoku.ac.jp

Abbreviations used: AD, Alzheimer's disease; BBB, blood–brain barrier; BSB, (trans, trans)-1-bromo-2,5-bis-(3-hydroxycarbonyl-4-hydroxy)styrylbenzene; CJD, Creutzfeldt–Jakob disease; DMSO, dimethylsulfoxide; FDDNP, 2-(1-[6-[(2-fluoroethyl)(methyl)amino]-2-naphthyl]ethylidene)malononitrile; GSS, Gerstmann–Strässler–Scheinker syndrome; ICR, Institute of Cancer Research; ID, injected dose; NT, not tested; PrP, prion protein; PrPres, protease-resistant PrP; PTA, phosphotungstic acid; PVDF, polyvinylidene difluoride; TSE, transmissible spongiform encephalopathy.

© 2006 The Authors
Journal Compilation © 2006 International Society for Neurochemistry,

Congo red and thioflavin T, are useful for detection of prion plaques and treatment of TSE (Ishikawa *et al.* 2004). These compounds, however, are limited in their ability because of inefficient brain uptake. Here we describe new compounds, styrylbenzoazole derivatives, which have been developed for practical use and analyzed for their PrP imaging ability, anti-prion activity, therapeutic efficacy, brain uptake and toxicity.

Materials and methods

Chemicals and experimental models

All of the test compounds were synthesized at Tanabe R & D (Saitama, Japan) and used freshly after being dissolved in 100% dimethylsulfoxide (DMSO).

Cultured cells were grown in Opti-MEM (Invitrogen, Carlsbad, CA, USA) supplemented with 10% fetal calf serum. As cellular models of TSE, we used mouse neuroblastoma (N2a) cells persistently infected with the RML strain (ScN2a) (Race *et al.* 1988) and six other prion-infected cell lines: N2a58 cells individually infected with the RML strain, the 22L strain (Nishida *et al.* 2000) and Fukuoka-1 strain (Ishikawa *et al.* 2004); N2a cells infected with the 22L strain; mouse hypothalamic cells (GT1-7) infected with the 22L strain (Milhavet *et al.* 2000); and mouse fibroblast cells (L929) infected with the RML strain (Vorberg *et al.* 2004).

Tg7 mice overexpressing hamster PrP (Race *et al.* 1995) and Tga20 mice overexpressing mouse PrP (Fischer *et al.* 1996) were also used. These mouse models were intracerebrally infected with 20 μL brain homogenate comprising 1% (w/v) of the 263K strain and the RML strain respectively. The Tg7 mice showed plaque-type PrP deposition between the cerebral cortex and hippocampus by 6 weeks after infection, followed by synaptic-type PrP deposition in the thalamus. The Tga20 mice showed similar pathological deposition, but plaques were not seen as frequently. Each mouse weighed ~30 g, and was maintained under deep ether anesthesia for minimum distress during all surgical procedures. Permission for the animal study was obtained from either the Animal Experiment Committee of Kyushu University or Tohoku University, Japan.

Brain uptake study

Test compounds were administered intravenously to Institute of Cancer Research (ICR) mice under ether anesthesia to determine initial brain uptakes. At 2 or 30 min after injection, the brains were removed, weighed and homogenized with saline. After centrifugation of the homogenate at 21 900 *g* for 10 min, the supernatant was applied to a conditioned C18 solid-phase extraction cartridge, and the compounds were eluted with methyl alcohol. Fluorescence was detected by high performance liquid chromatography with a fluorescence detector as reported previously (Okamura *et al.* 2005), and the percentage of injected dose per gram (%ID/g) was used as a measure of the level of the compounds in the brain.

In vitro PrP imaging in sections

Autopsy-diagnosed brain samples from cases of Gerstmann–Strässler–Scheinker syndrome (GSS) ($n = 2$), sporadic CJD ($n = 5$), iatrogenic dura CJD with synaptic PrP deposition ($n = 1$) and non-TSE control cases with amyloid lesions [Alzheimer's disease (AD), $n = 2$] or without amyloid lesions (cerebral infarction, $n = 1$) were obtained from the Department of Neuropathology, Kyushu University, Japan. After fixation in 10% buffered formalin for 2 weeks, each sample of TSE was immersed in 98% formic acid for the reduction of prion infectivity, embedded in paraffin and cut into sections 7 μm thick. Sections of a variant CJD case were kindly provided by Dr James W. Ironside of the CJD Surveillance Unit, Edinburgh, UK. For neuropathological staining, deparaffinized sections were immersed in 1% Sudan black solution to quench tissue autofluorescence. They were then incubated for 30 min in 1-μM solutions of the test compounds, rinsed with distilled water and examined under a fluorescence microscope (DMRXA; Leica Instruments, Wetzler, Germany) with a UV or FITC filter set.

For comparison, each section was subsequently immunoassayed for PrP as described previously (Doh-ura *et al.* 2000). Briefly, the sections were treated with a hydrolytic autoclave and incubated with a rabbit primary antibody, c-PrP, which was raised against a mouse PrP fragment, amino acids 214–228 (1 : 200; Immuno-Biological Laboratories, Gunma, Japan), followed by incubation with a horseradish peroxidase-conjugated secondary antibody (1 : 200; Vector Laboratories, Burlingame, CA, USA). The reaction product was developed with 3,3′-diaminobenzidine tetrahydrochloride solution and counterstained with hematoxylin. Paraffin-embedded brains of experimental animals were similarly investigated.

In vivo PrP imaging in model animals

BF-168 (molecular weight 312.34) dissolved in 10% DMSO was administered intravenously (0.5–5 mg/kg body weight) into Tg7 mice at 6–7 weeks after injection when the mice showed no apparent clinical signs of TSE. As controls, vehicle alone was similarly injected into infected mice, and BF-168 was administered into uninfected mice. The animals were killed at various time points, and the brains were rapidly frozen and cut into coronal sections 10 μm thick using a cryostat (CM3050; Leica Instruments). The sections were thaw-mounted on slides, dried and coverslipped. They were examined under a fluorescence microscope and further analyzed immunohistochemically as described above.

In vitro treatment in cell cultures

Abnormal PrP formation was assayed by the content of protease-resistant PrP (PrPres) in cellular models of TSE as described previously (Caughey and Raymond 1993). Each compound was added at the designated concentrations when cells were passaged at 10% confluence, while maintaining the final concentration of DMSO in the medium at < 0.5%. The cells were allowed to grow to confluence and lysed with lysis buffer (0.5% sodium deoxycholate, 0.5% Nonidet P-40, phosphate-buffered saline). For analysis of PrPres, samples were digested with 10 μg/mL proteinase K for 30 min, and the digestion was stopped with 0.5 mM phenylmethylsulfonyl fluoride. The samples were centrifuged at 100 000 *g* for 30 min, and pellets were resuspended in 1 × sample loading buffer and boiled. For analysis of cellular PrP in N2a cells, cell lysates were mixed directly with a quarter volume of 5 × sample loading buffer and boiled. These samples were separated by electrophoresis on a 15% Tris–glycine–sodium dodecyl sulfate polyacrylamide gel and electroblotted on to a polyvinylidene difluoride (PVDF) filter (Millipore, Bedford, MA, USA). PrP was detected using a monoclonal antibody, SAF83 (1 : 5000; SPI-BIO, Massy, France), followed by an alkaline phosphatase-conjugated

© 2006 The Authors

goat anti-mouse antibody (1 : 20 000; Promega, Madison, WI, USA). Immunoreactive blots were visualized with CDP-Star detection reagent (Amersham, Piscataway, NJ, USA). More than two independent assays were performed in each experiment and signals were analyzed using image analysis software. The approximate concentration of the compound giving 50% inhibition of PrPres formation, relative to the vehicle-treated control (IC_{50}), was estimated by signal intensity. To control for the detection limits of western blotting, we performed additional experiments utilizing sodium phosphotungstic acid (PTA) precipitation, which is the most sensitive technique presently available to detect PrPres (Safar *et al.* 1998). The PTA precipitation was undertaken on cell lysates of ScN2a treated with BF-168 at a designated concentration. The resulting pellets were collected by centrifugation and then analyzed by immunoblotting as described above.

In vivo treatment in model animals

BF-168 solution (4 mg/kg body weight) or vehicle alone was injected intravenously to experimental animals ($n = 5$) once a week. The treatment was started at 2 weeks after injection for Tg7 mice and at 4 weeks after injection for Tga20 mice, and repeated for 4 weeks. A continuous subcutaneous infusion of BF-168 was also given to Tga20 mice ($n = 5$) using an Alzet osmotic pump (Durect, Cupertino, CA, USA). In accordance with the manufacturer's instructions, each pump was filled with BF-168 solution at the designated doses and placed in a subcutaneous area of the back at 4 weeks after injection. The animals showed no apparent adverse effects of the treatment and were monitored 5 days a week until obvious clinical signs appeared. Statistical significance was analyzed by one-way ANOVA followed by Scheffé's method for multiple comparisons.

Results

Brain uptake and toxicity

We designed and synthesized novel styrylbenzoxazole derivatives (Table 1), styrylbenzothiazole and styrylbenzoimidazole derivatives (Table 2) with more efficient permeability of the BBB and less toxicity. Values for brain uptake at 2 min after intravenous injection of the compounds were in the 2.4–17.0%ID/g range, indicating a satisfactory level for imaging probes. Their washouts from the brain varied, with the ratio of %ID/g at 2 min to that at 30 min after injection ranging from 1.0 to 56.9. Acute toxicity was tested by administering each compound intravenously at ~10 mg/kg body weight into normal ICR mice. No apparent toxic effect was observed with any of the compounds tested.

PrP imaging ability

Imaging of abnormal PrP deposition by the compounds was first performed in brain sections of human TSE. The compounds fluorescently labeled most of the PrP plaques in cerebellar cortices of both GSS cases (Fig. 1a, representative data). Among sections from the sporadic CJD cases, PrP deposition was labeled only in a case with plaques (Fig. 1c). In the cerebral cortex from the variant CJD case, large core plaques were detectable, whereas the majority of immunopositive aggregates were not labeled (Fig. 1e). In contrast, no fluorescence signal was identified in sections from the dura CJD case or the other sporadic CJD cases that

Table1 Chemical structure, PrPres inhibition and brain uptake of styrylbenzoxazole derivatives including BF-168

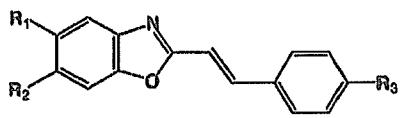

Compound	R_1	R_2	R_3	IC_{50} (nM)[a]	Brain uptake (%ID/g)[b] 2 min	Brain uptake (%ID/g)[b] 30 min	Ratio of 2 to 30 min brain uptake
BF-168	H	$O(CH_2)_2F$	$NH(CH_3)$	0.4	3.9[c]	1.6	2.4
BF-125	H	H	$N(C_2H_5)_2$	10.2	3.0	3.0	1.0
BF-133	F	H	$N(CH_3)_2$	1.6	5.5	3.8	1.4
BF-135	NO_2	H	$N(CH_3)_2$	< 1	NT[d]	NT	-
BF-140	F	H	NH2	< 1	5.5	1.1	5.0
BF-145	F	H	$NH(CH_3)$	< 1	4.4	1.6	2.8
BF-148	H	F	$N(CH_3)_2$	< 1	NT	NT	-
BF-165	H	H	$NH(CH_3)$	7.1	7.2	NT	-
BF-169	H	OH	$NH(CH_3)$	2.4	NT	NT	-
BF-173	I	H	NH_2	2.2	NT	NT	-
BF-180	I	H	$NH(CH_3)$	8.5	2.4	1.8	1.3
BF-191	H	H	Cl	1.8	12.0	1.7	7.1
BF-208	H	H	F	< 1	11.0	0.53	20.8
N-282	H	H	$N(CH_3)_2$	2.1	4.0	1.7	2.4
N-407	H	H	H	< 1	17.0	0.99	17.2

[a]IC_{50}, approximate concentration of a compound giving 50% inhibition of PrPres formation relative to the control in ScN2a cells.
[b]%ID/g, percentage of injected dose per gram in the brains of normal mice.
[c]already reported in the previous work (Okamura *et al.*, 2004).
[d]NT, not tested.

© 2006 The Authors

Table 2 Chemical structure, PrPres inhibition and brain uptake of styrylbenzothiazole and styrylbenzoimidazole derivatives

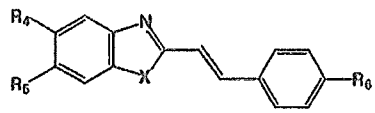

Compound	X	R_4	R_5	R_6	IC_{50} (nM)[a]	Brain uptake (%ID/g)[b] 2 min	Brain uptake (%ID/g)[b] 30 min	Ratio of 2 to 30min brain uptake
BF-124	S	H	H	$N(C_2H_5)_2$	18.1	2.4	2.5	1.0
BF-162	S	F	H	$N(CH_3)_2$	1.4	NT[c]	NT	-
N-276	S	H	H	$N(CH_3)_2$	< 1	NT	NT	-
N-438	S	H	H	H	< 1	11.0	2.0	5.5
BF-126	NH	H	H	$N(C_2H_5)_2$	21	7.2	0.16	45
BF-166	NH	F	H	$N(C_2H_5)_2$	1.1	NT	NT	-
N-457	NH	H	H	Cl	< 1	7.1	0.21	33.8
N-491	NH	H	H	H	1.9	7.4	0.13	56.9

[a]IC_{50}, approximate concentration of a compound giving 50% inhibition of PrPres formation relative to the control in ScN2a cells.
[b]%ID/g, percentage of injected dose per gram in the brains of normal mice.
[c]NT, not tested.

included perivacuolar and/or synaptic PrP deposition (data not shown). Background staining was barely observed after rinsing off the excess compound. Immunohistochemical analysis of PrP revealed that the compounds achieved high-specificity labeling (Figs 1b, d and f). The compounds displayed no signal in control sections without amyloid lesions (data not shown).

Similar results were observed in experimental mice. PrP plaques were specifically labeled in brain sections of Tg7 mice infected with the 263K strain, and there was no PrP immunopositive reaction or fluorescence signal in brain sections of uninfected mice (data not shown). We performed *in vivo* experiments using presymptomatic Tg7 mice at a later stage of TSE. A typical image is shown in Fig. 1(g); peripheral administration of BF-168 fluorescently labeled plaques in the cerebral white matter, indicating that the compound efficiently entered the brain and bound to coarse PrP deposits. Subsequent immunostaining verified the specificity and sensitivity for PrP (Fig. 1h). Non-specific staining, such as cerebrovascular labeling, was occasionally observed at 4 h after injection of 5 mg/kg BF-168, but not after 8 h or more. The stability of the fluorescence signals was examined at various time points up to 24 h after injection and the dye–PrP complex remained visible at the latest time. In contrast, there was no significant labeling after an injection of BF-168 into uninfected animals, or after an injection of vehicle alone to terminally ill Tg7 mice. Similar results were obtained for Tga20 mice infected with the RML strain, although plaques were less frequently detected (data not shown).

Anti-prion activity *in vitro*

The anti-prion activities of the compounds were investigated using ScN2a cells, which are most commonly used for drug screening for TSE treatment. Styrylbenzoxazole derivatives, including BF-168, were evaluated and confirmed to inhibit PrPres formation with IC_{50} values in the nanomolar or subnanomolar range (Fig. 2a and Table 1). Styrylbenzothiazole and styrylbenzoimidazole derivatives were similarly potent, in a dose-dependent manner, within a non-toxic dose range (~10 μM) (Table 2). Treatment with vehicle alone showed no inhibitory effect compared with untreated controls (Fig. 2a). We utilized PTA precipitation, which increases the sensitivity of western blotting, and confirmed the potency of BF-168 at a concentration of 10 times the IC_{50}. Furthermore, radiographic film was exposed to the blotted PVDF membranes for 10 times longer than usual before developing. No significant signals were visualized, whereas bands representing the vehicle-treated control were so strong as to be already saturated (Fig. 2b). To determine whether the efficacy was transient, ScN2a cells treated with 10 nM BF-168 were further cultured for 2 weeks in the absence of BF-168. PrPres signals never reappeared, even through four passages after discontinuation of the treatment (Fig. 2c). To exclude the possibility of interference with immunodetection, BF-168 solution at a final concentration of 10 nM was added to a lysate of untreated ScN2a cells before proteinase K digestion. PrP signals were not affected (data not shown). Nor was any alteration observed in cellular PrP level of N2a cells after treatment with 10 nM BF-168 (Fig. 2d).

To investigate whether the efficacy of the compounds depends on pathogen strain, we tested BF-168 in three N2a58 cell lines individually infected with different strains. As shown in Table 3, BF-168 was only effective in N2a58 cells infected with the RML strain, although the inhibitory activity was not as strong as in ScN2a cells (~1 μM). In contrast, BF-168 was ineffective in the same N2a58 cells infected with the 22L or Fukuoka-1 strains up to 10 μM, a dose at which the compound showed host cytotoxicity.

© 2006 The Authors

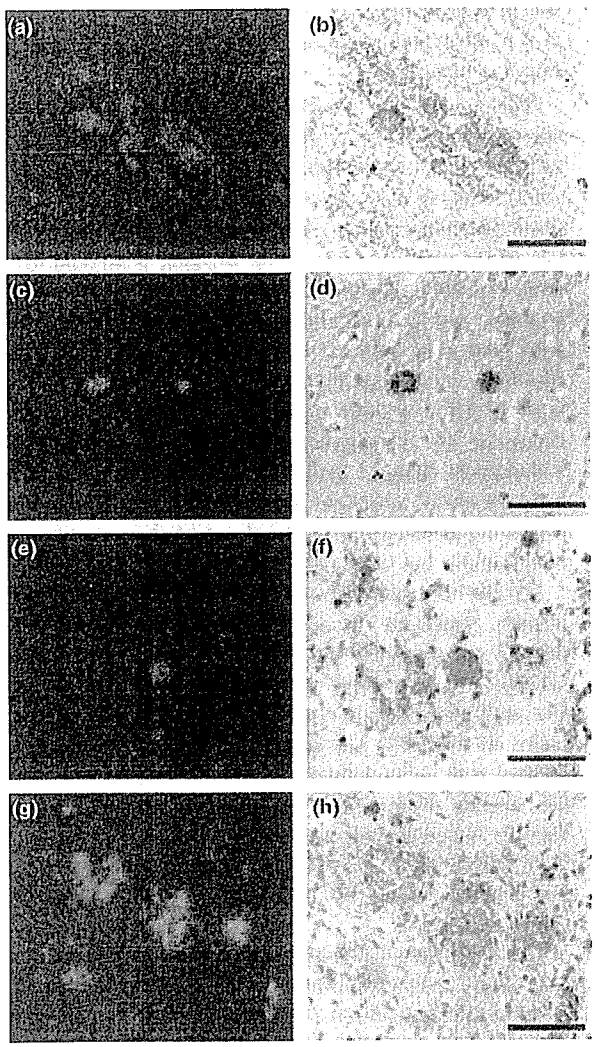

Fig. 1 PrP imaging *in vitro* and *in vivo*. BF-168 fluorescently labeled PrP deposition in a cerebellar section from the case of GSS (a), and in cerebral sections from cases of sporadic CJD with plaques (c) and variant CJD (e). Similar results were obtained from the brains of living TSE-infected mice that were intravenously injected with BF-168 solution (0.5 mg/kg). BF-168 detected PrP deposition in the cerebral white matter between the cortex and hippocampus (g). Sections (a, c, e and g) were subsequently immunoassayed for PrP (b, d, f and h). Bars represent 100 μm (a–f) and 25 μm (g and h).

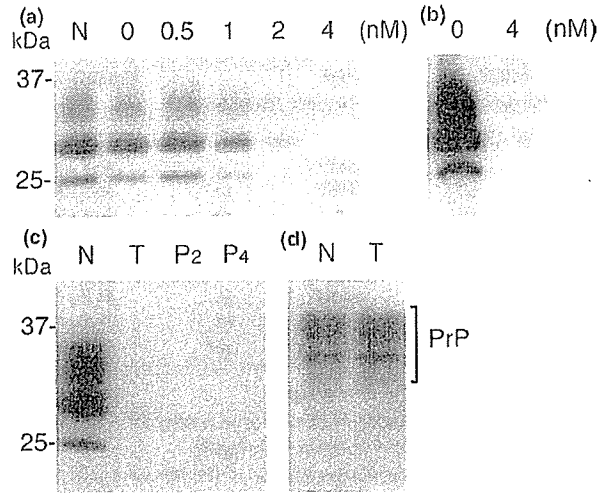

Fig. 2 Effects of BF-168 on PrP expression in ScN2a and N2a cells. BF-168 was added at the designated concentrations to freshly passaged cells. PrPres formation in ScN2a cells was inhibited in a dose-dependent manner (a). To exclude the sensitivity limit of immunoblotting, ScN2a cells treated with 4 nM BF-168 were also analyzed by sodium PTA, and no significant signals were visualized (b). ScN2a cells treated with 10 nM BF-168 were maintained for an additional four passages, and the PrPres signal was not restored in the absence of BF-168 (c). PrP expression was not affected in N2a cells that were grown in the presence of 10 nM BF-168 (d). Lane N, untreated cells; lane 0, cells treated with vehicle alone; lane T, cells treated with 10 nM BF-168; lanes P_2 and P_4, cells following two and four passages after treatment respectively. Bars on the left indicate molecular size markers at 37 and 25 kDa.

Table 3 Anti-prion activities (IC_{50}) of BF-168 in various types of TSE-infected cells

Host cells	Pathogen strains		
	RML	22L	Fukuoka-1
N2a	0.4 nM	None[a]	–[b]
N2a58	~1 μM	None	None
L929	~10 nM	–	–
GT1-7	–	None	–

[a]None, no significant PrPres inhibition up to 10 μM, a dose that affect the rate of cell growth.
[b], not available.

Furthermore, we established L929 cells stably infected with the RML strain. BF-168 inhibited PrPres formation in the RML-infected L929 cells with an IC_{50} in the nanomolar range. We also tested potency against the 22L strain in two other cell lines, N2a and GT1-7 cells. BF-168 was ineffective in either cell line infected with the 22L strain. Other compounds tested here demonstrated similar results (data not shown). These results suggest that the styrylbenzoxazole derivatives exert their inhibitory activity on PrPres formation in a strain-dependent, but not a host cell-dependent, manner.

Therapeutic efficacy *in vivo*

The therapeutic activity of the compounds *in vivo* was assayed in two different mouse models using BF-168 as a representative. Treatment was initiated 2–4 weeks after TSE infection and repeated once a week for 4 weeks. The dosage at a single administration corresponded to a dose sufficient to detect PrP plaques. As shown in Table 4, there was no

© 2006 The Authors
Journal Compilation © 2006 International Society for Neurochemistry,

Table 4 Effects of BF-168 treatment on intracerebrally TSE-infected mice

Mouse - pathogen strain	*n*	Dose (mg/kg/week)	Administration	Incubation period Mean ± SD (days)
Tg7 - 263K				
	7	Control	-	49.4 ± 1.9
	5	Vehicle	i.v.[a]	50.2 ± 4.1
	5	4	i.v.	52.2 ± 2.6
Tga20 - RML				
	7	Control	-	66.6 ± 1.6
	5	Vehicle	i.v.	64.8 ± 1.6
	5	4	i.v.	72.2 ± 2.5*
	5	10	s.c.[b]	66.0 ± 3.1

* $p < 0.001$ versus the oher groups.

[a]i.V., intravenous injection of BF-168 once a week for 4 weeks from 2 weeks p.i. for Tg7, or 4 weeks p.i. for Tga20.

[b]s.c., continous subcutaneous infusion of BF-168 for 4 weeks from 4 weeks p.i.

significant difference in incubation periods between groups of Tg7 mice infected intracerebrally with the 263K strain, with or without treatment. In contrast, intravenous injection with 4 mg/kg BF-168 significantly prolonged the incubation period (~ 11.4%) of Tga20 mice intracerebrally infected with the RML strain.

In another trial, we used osmotic pumps filled with BF-168 solution, assuming that the route of administration is a key issue. The pump worked continuously for 4 weeks, and the total dosage for the duration was selected to correspond to two to three times that administered intravenously. Subcutaneous infusion of BF-168, however, did not prolong incubation periods of Tga20 mice intracerebrally infected with the RML strain (Table 4). There was no significant difference in incubation period in either group of infected mice between untreated controls and controls treated with vehicle alone.

Discussion

Our results show that styrylbenzoazole derivatives represent candidates for imaging probes as well as therapeutic drugs for TSE. It has been increasingly necessary to develop minimally non-invasive methods for recognizing early clinical infection and evaluating treatment of TSE. We have already focused on two β-amyloid imaging probes and reported them as potential agents for TSE (Ishikawa *et al.* 2004). The problem is, however, that they seemed to have practical limitations because of inadequate brain uptake and washout. Here, we confirmed that novel styrylbenzoazole derivatives clearly labeled PrP plaques *in vitro* and BF-168, the parent compound, entered the brain and labeled PrP plaques *in vivo*, even at a 20-fold lower dose than the probes we previously reported. In brain uptake studies, all of the compounds showed BBB permeability with >1%ID/g, which is proposed to be sufficient for neuroimaging probes. The background staining of 0.5 mg/kg BF-168 was almost absent at 4 h after administration, suggesting excellent clearance from the brain.

Most of styrylbenzoazole derivatives labeled β-amyloid aggregates in AD specimens in this study (data not shown) as well as in the previous study on Alzheimer's (Okamura *et al.* 2004). This is also observed with 2-(1-[6-[(2-fluoroethyl)(methyl)amino]-2-naphthyl]ethylidene)malononitrile (FDDNP), one of the promising agents for imaging β-amyloid deposition. FDDNP has been reported to label PrP plaques in brain sections, and is a candidate for imaging PrP deposition (Bresjanac *et al.* 2003). These findings imply lack of disease specificity, but the compounds should still be useful for some types of TSE, because anatomical distributions of amyloid deposition are characteristically different between diseases. Pathological changes including amyloid deposition of AD brain are always observed in the hippocampus but not in the cerebellum, whereas those of TSE tend to be absent from the hippocampus but to be demonstrated in the cerebellum.

Styrylbenzoazole derivatives detected predominantly PrP plaques, especially in specimens of sporadic CJD with plaques and variant CJD. However, their ability to detect synaptic or perivacuolar PrP deposition remains inconclusive, until more sensitive investigations, such as autoradiography, are available. The compounds tested in this study can be used with radionuclides. ^{18}F-radiolabeled BF-168, which has already been employed for labeling of β-amyloid deposits including both neuritic and diffuse plaques in AD brain (Okamura *et al.* 2004), may be a suitable tool for investigating whether PrP deposition, other than plaque type, can be detected.

This study demonstrated that styrylbenzoazole derivatives have more potent anti-prion activity than the amyloid imaging probes reported previously (Ishikawa *et al.* 2004). Although the neuropathological processes remain unclear, one of the most likely strategies for TSE treatment is a small-molecule drug that can enter the brain and inhibit abnormal PrP formation. It is important to emphasize that styrylbenzoazole derivatives have a wide concentration safety margin, and some were effective even at subnanomolar doses in ScN2a cells. Dozens of drug candidates for TSE have been reported to date but, as far as we know, the most potent inhibitor class for abnormal PrP formation in ScN2a cells is specific blocking antibodies with an IC_{50} in the nanomolar range (Peretz *et al.* 2001).

BF-168 showed no apparent alteration in cellular PrP expression level in N2a cells, and also labeled abnormal PrP deposition both *in vitro* and *in vivo*. These data suggest that styrylbenzoazole derivatives might interact directly with abnormal PrP molecules to block the conversion of normal to abnormal PrP. The structure–activity relationship, examined by introducing side-chain or functional groups into the benzoazole and/or benzene rings, demonstrates that the inhibitory potency is not always the same, even among

© 2006 The Authors
Journal Compilation © 2006 International Society for Neurochemistry.

closely related compounds (data not shown). Although we could not obtain any insight into inhibitory mechanisms, the efficacy of BF-168 was dependent on pathogen strain, and this is consistent with our previous work using three types of cell lines (Ishikawa *et al.* 2004). In an attempt to further explore strain dependency, we tested three different pathogen strains in one host cell line, and three different host cell lines with one pathogen strain. BF-168 inhibited abnormal PrP formation in all three types of RML-infected cells, including ScN2a cells. By contrast, BF-168 did not demonstrate any inhibitory activity in the 22L- or Fukuoka-1-infected cells. It is well known that prion strains differ in their biological profiles such as the degree of glycosylation and the conformation of PrP molecules. In the imaging experiments we confirmed that the compound bound to a certain type of abnormal PrP aggregates. Thus, it was assumed that the therapeutic efficacy might be based on blocking certain interactions between normal and abnormal PrP, and that BF-168 might recognize the PrP conformation. However, considering a discrepancy in the *in vivo* experiment between PrP imaging and treatment using infected Tg7 mice, these inferences remain unsupported and the precise mechanism of the strain-dependent efficacies needs to be elucidated.

Kocisko *et al.* (2004) reported that anti-prion activity *in vitro* does not always correlate with that *in vivo*. With *in vivo* testing, there are many variables, such as inoculation route, dosing protocol and pathogen strain. The efficacy differed according to the BF-168 administration route in Tga20 mice, even though the dose administered subcutaneously for the same duration was no less than that administered intravenously. This might be due to differences in stability and clearance of BF-168 in relation to the route of administration.

Most previous therapeutic investigations showed a significant benefit *in vivo* when the treatment was started before, or soon after, peripheral TSE infection. Although the efficacy of BF-168 was limited, it is noteworthy that we obtained significant results with peripheral administration at a later stage of the intracerebral infection. In addition, BF-168 showed excellent brain uptake and binding affinity towards PrP aggregates *in vivo*, even at a low dose, suggesting that the compound should be a good imaging probe for clinical use. In the treatment of infected Tga20 mice, BF-168 showed almost the same prolongation of the incubation period but with a 10-fold smaller dose than (trans, trans)-1-bromo-2,5-bis-(3-hydroxycarbonyl-4-hydroxy)styrylbenzene (BSB), which we reported previously as one of the amyloid imaging probes applicable for TSE (Ishikawa *et al.* 2004). BF-168 showed a low IC_{50} of 0.4 nM in treatment of ScN2a cells, whereas the IC_{50} of BSB was more than 1000-fold higher (1.4 μM). We decided the dosing protocol for our experimental animals from *in vitro* data, including the ratio of these IC_{50} values, and from an *invivo* imaging experiment in which 0.1 mg BF-168 per injection was enough to detect PrP deposition. It is also necessary to consider washout of the compound from the brain. Further studies are required to examine issues such as dose–response relationships, administration time and dosing conditions. Furthermore, there was a problem in that administration frequency was limited because animal tail tissue was damaged by repetitive intravenous injections. In addition, it should be investigated whether compounds with slower washout from the brain are more suitable as therapeutic agents.

In conclusion, styrylbenzoazole derivatives efficiently entered the brain and labeled pathological PrP deposition, and demonstrated some anti-prion activities both *in vitro* and *in vivo*. Although their efficacy depended on the pathogen strain, these are a new class of compounds with potential as therapeutic drugs and imaging probes for TSE.

Acknowledgements

This study was supported by grants to KD from the Ministry of Health, Labour and Welfare (H16-kokoro-024) and the Ministry of Education, Culture, Sports, Science and Technology 13557118, 14021085, Japan. The authors thank Dr James W. Ironside of the CJD Surveillance Unit, Edinburgh, UK, for providing the variant CJD specimens.

References

Bresjanac M., Smid L. M., Vovko T. D., Petric A., Barrio J. R. and Popovic M. (2003) Molecular-imaging probe 2-(1-[6-[(2-fluoroethyl)(methyl) amino]-2-naphthyl]ethylidene) malononitrile labels prion plaques *in vitro*. *J. Neurosci.* **23**, 8029–8033.

Brown P., Preece M., Brandel J. P. *et al.* (2000) Iatrogenic Creutzfeldt–Jakob disease at the millennium. *Neurology* **55**, 1075–1081.

Caughey B. and Raymond G. J. (1993) Sulfated polyanion inhibition of scrapie-associated PrP accumulation in cultured cells. *J. Virol.* **67**, 643–650.

Doh-ura K., Mekada E., Ogomori K. and Iwaki T. (2000) Enhanced CD9 expression in the mouse and human brains infected with transmissible spongiform encephalopathies. *J. Neuropathol. Exp. Neurol.* **59**, 774–785.

Fischer M., Rulicke T., Raeber A., Sailer A., Moser M., Oesch B., Brandner S., Aguzzi A. and Weissmann C. (1996) Prion protein (PrP) with amino-proximal deletions restoring susceptibility of PrP knockout mice to scrapie. *EMBO J.* **15**, 1255–1264.

Ishikawa K., Doh-ura K., Kudo Y., Nishida N., Murakami-Kubo I., Ando Y., Sawada T. and Iwaki T. (2004) Amyloid imaging probes are useful for detection of prion plaques and treatment of transmissible spongiform encephalopathies. *J. Gen. Virol.* **85**, 1785–1790.

Kocisko D. A., Morrey J. D., Race R. E., Chen J. and Caughey B. (2004) Evaluation of new cell culture inhibitors of protease-resistant prion protein against scrapie infection in mice. *J. Gen. Virol.* **85**, 2479–2483.

Milhavet O., McMahon H. E., Rachidi W. *et al.* (2000) Prion infection impairs the cellular response to oxidative stress. *Proc. Natl Acad. Sci. USA* **97**, 13 937–13 942.

Nishida N., Harris D. A., Vilette D., Laude H., Frobert Y., Grassi J., Casanova D., Milhavet O. and Lehmann S. (2000) Successful transmission of three mouse-adapted scrapie strains to murine neuroblastoma cell lines overexpressing wild-type mouse prion protein. *J. Virol.* **74**, 320–325.

© 2006 The Authors
Journal Compilation © 2006 International Society for Neurochemistry,

Okamura N., Suemoto T., Shimadzu H. *et al.* (2004) Styrylbenzoxazole derivatives for *in vivo* imaging of amyloid plaques in the brain. *J. Neurosci.* **24**, 2535–2541.

Okamura N., Suemoto T., Furumoto S. *et al.* (2005) Quinoline and benzimidazole derivatives: candidate probes for *in vivo* imaging of tau pathology in Alzheimer's disease. *J. Neurosci.* **25**, 10 857–10 862.

Peretz D., Williamson R. A., Kaneko K. *et al.* (2001) Antibodies inhibit prion propagation and clear cell cultures of prion infectivity. *Nature* **412**, 739–743.

Prusiner S. B. (1991) Molecular biology of prion diseases. *Science* **252**, 1515–1522.

Race R. E., Caughey B., Graham K., Ernst D. and Chesebro B. (1988) Analyses of frequency of infection, specific infectivity, and prion protein biosynthesis in scrapie-infected neuroblastoma cell clones. *J. Virol.* **62**, 2845–2849.

Race R. E., Priola S. A., Bessen R. A., Ernst D., Dockter J., Rall G. F., Mucke L., Chesebro B. and Oldstone M. B. (1995) Neuron-specific expression of a hamster prion protein minigene in transgenic mice induces susceptibility to hamster scrapie agent. *Neuron* **15**, 1183–1191.

Safar J., Wille H., Itri V., Groth D., Serban H., Torchia M., Cohen F. E. and Prusiner S. B. (1998) Eight prion strains have PrP(Sc) molecules with different conformations. *Nat. Med.* **4**, 1157–1165.

Vorberg I., Raines A., Story B. and Priola S. A. (2004) Susceptibility of common fibroblast cell lines to transmissible spongiform encephalopathy agents. *J. Infect. Dis.* **189**, 431–439.

Will R. G., Ironside J. W., Zeidler M. *et al.* (1996) A new variant of Creutzfeldt–Jakob disease in the UK. *Lancet* **347**, 921–925.

© 2006 The Authors
Journal Compilation © 2006 International Society for Neurochemistry.